Forest Fire Research & Wildland Fire Safety, Viegas (ed.)

Burned land mapping using NOAA-AVHRR and TERRA-MODIS

M. Pilar Martín and Ricardo Díaz Delgado
Consejo Superior de Investigaciones Científicas, Pinar 2, 28006 Madrid, Spain

Emilio Chuvieco and Gemma Ventura
Universidad de Alcalá. Departamento de Geografía, Colegios 2, 28880 Alcalá de Henares, Spain

Keywords: remote sensing, AVHRR, MODIS, burned land mapping

ABSTRACT: Spatial and temporal analysis of MODIS and AVHRR images have been carried out to discriminate burned areas from other land covers. Spatial and temporal analysis were performed based on statistical separability and temporal changes. The objective of these analysis was to find out the most sensitive bands for burned land mapping in order to design spectral indices better adapted to the discrimination of burned areas. MODIS images were found to be more sensitive than AVHRR images, caused by both the better spatial and spectral resolution. The near infrared and short-wave infrared bands were found more adequate than visible channels to separate burned areas from other land covers, although the thermal channels of AVHRR also contributed significantly to separability indices. This may be caused by the short time span between fire occurrence and image acquisition. These analysis will be the basis to derive global mapping of burned areas from coarse resolution sensors, such as MODIS and AVHRR.

1 INTRODUCTION

A well-structured decision making system for the rational management of forest fires requires a complete, accessible and accurate spatial database of burnt areas. Appropriate statistics on fire incidence on a permanent basis, will help fire managers to better understand the fire problem including the reasons of fire occurrence and spreading (Koutsias and Karteris, 1998). Burnt land maps require consistent, quick and wide-coverage methods, which should ensure the appropriate temporal and spatial inventory of fire affected areas.

Satellite remote sensing provides periodic digital data from different spectral regions. The use of remote sensing methods in burned land assessment has grown notably in the last decade, as reported in the vast literature available on this application (see, for instance, the works referred in Chuvieco, 1999). A simple classification of recent papers makes it possible to highlight three lines of research:

a) Applications of new sensors, such as SPOT-Vegetation, DMSP-OLE and Terra-Modis, attempting to either overcome the limitations found using Landsat or NOAA images or complement their advantages (Fraser and Landry, 2000; Landry et al., 1995). This is one of the most active lines, since the new generation of hyperspectral sensors will critically modify the spectral information available for burned land mapping.

b) Development or adaptation of methods for burned land discrimination, mainly interferometry, spectral unmixing, logistic regression and change detection analysis. Within this approach, the main objective is to test new processing algorithms in order to improve the identification of areas

affected by fires (Bruzzone and Fernández-Prieto, 2000; Fraser et al., 2000; Koutsias and Karteris, 1998; Koutsias et al., 2000).

c) Generation of new indices adapted to burned land areas. In this case, the goal has been to define spectral indices that can characterize the spectral behavior of burned areas more clearly. Testing spectral indices for burned land discrimination was undertaken by López and Caselles (1991) using Landsat-TM data. These authors emphasized the adequacy of NIR-SWIR spectral domain for this purpose, which was later demonstrated by other authors also: Pereira (1999) using AVHRR data, and Trigg and Flasse (2001) from spectro-radiometric measurements. Martín (1998) questioned the convenience of standard vegetation indices based on red and near infrared reflectance for burned area mapping, and proposed a new index specifically designed for this application, based on NOAA-AVHRR images.

At global scales, most of the studies on burned land mapping at regional/global scales had been accomplished using NOAA-AVHRR (*Advanced Very High Resolution Radiometer*) and ATSR (*Along-Track Scanning Radiometer*) images. However, the arrival of a new generation of spaceborne sensors designed for environmental studies, such as Terra-MODIS (*Moderate-Resolution Imaging Spectroradiometer*) and Envisat-MERIS (*Medium Resolution Imaging Spectrometer*) should offer substantial benefits for burned land mapping due to the improved spectral and spatial resolution over NOAA-AVHRR images. Adapting methods previously derived for those images are required to better exploit potentials of new satellite sensors.

2 OBJECTIVES

The objective of this paper is to test the discrimination potential of Terra-MODIS images for burned land mapping, analysing their performance over NOAA-AVHRR data. This analysis is focused on global scales and therefore only considers large fires (above 100 hectares). Some examples extracted from recent fires in Spain are presented.

3 METHODOLOGY

3.1 *Pre-processing*

NOAA-AVHRR and Terra-MODIS images were acquired for the summer of 2001 for the whole Iberian Peninsula. The former were received by the HRPT station located at the department of Geography of University of Alcalá (http://www.geogra.uah.es/NOAA/NOAA.htm), while the latter were downloaded from the Terra-MODIS webpage (http://modis.gsfc.nasa.gov/). Spectral and spatial resolution characteristics of both sensors are included in table 1. Although the MODIS sensor also include thermal channels, only reflectance bands have been used in this work, since they provide better spatial resolution (250m the first two, and 500m from the 3rd to the 7th. The first two bands were reprojected to 500m to maintain a common spatial resolution in all bands.

The AVHRR images were georeferenced to UTM projection using navigation orbital models, while the MODIS were converted to this projection from the NASA projected format. Multitemporal fitting of AVHRR images was improved by using a semi-automatic approach based on a library of control point windows. This algorithm finds matching points in the first-order corrected images with respect to a reference image by maximizing correlation in the digital values spatial patterns.

Table 1: AVHRR and MODIS characteristics

Bands		AVHRR[1]	MODIS[2]
1	Wavelength (μm)	0.58 – 0.68	0.62 – 0.67
2		0.72 – 1.10	0.841 – 0.876
3		1.58 –1.64	0.459 – 0.479
4		10.3 –11.3	0.545 – 0.565
5		11.5 – 12.5	1.23 – 1.25
6			1.628 – 1.652
7			2.105 – 2.155
Spatial resolution		1.1 x 1.1 km	500 x 500 m

(1) Diurnal pass of AVHRR/3
(2) Only the first channels with higher resolution have been processed

Before the geometric correction was performed, raw digital values were converted to reflectance and brightness temperature using calibration coefficients provided by NOAA. This transformation makes it possible to compare values from two different sensors, since they are expressed in physical units. The analysis was performed with all 5 AVHRR channels, while for MODIS data only the shorter wavelengths were considered (channels 1 to 7, which range from 0.4 to 2.2 μm).

Taken into account the important factors of noise for the daily images (cloudiness, non-vertical observation, atmospheric scattering and so on), in this paper we have only worked with multidate composites. For MODIS data, the composites were derived using a standard procedure of NASA, which includes atmospheric and bi-directional reflectance corrections and is recommended for land applications (http://modis.gsfc.nasa.gov/data/dataprod/accuracy/mod09.html).

As far as the AVHRR images concern, the composites were based on two criteria: maximum surface temperature and minimum nadir observation angle. The former served to eliminate clouds and cloud shadows, preserving burned areas in case of having fires occurring during the composite period; the second one chooses the most vertical pixel, which should be less affected by atmospheric absorption and artefacts derived from observation geometry. The criteria finally chosen selects the most vertical observation from the three highest temperatures of the composite period. The figure 1 shows the differences between this procedure of obtaining multitemporal composites and the traditional procedure (named Maximum Value Composites, MVC), which chooses for each pixel the date that maximises the NDVI (*Normalized Difference Vegetation Index*). Several authors have shown that the MVC is not very appropriate for burned land mapping, since the NDVI values of a burned area are quite low and, therefore, maximizing this value will rarely retain the pixel affected by a fire (Martín and Chuvieco, 1998; Pereira et al., 1999). The figure is centered upon a large forest fire that affected the Western plateau of Spain in late July, 2001 (circled in red). The fire is clearly observable in the TS-Nadir composite, while difficult to differentiate in the composite performed with the MVC criterion.

3.2 *Spatial analysis*

To measure the discrimination ability of each spectral index, normalized distances (z) and average transformed divergences (TD) were computed for AVHRR and MODIS temporal composite images after the fire. These measurements were calculated using training sites of well characterized land covers extracted from the CORINE-land cover database.

Discrimination power of each band was measured by the average z distances from burned areas to all other land cover types, as well as the TD values between pair of classes (burned areas and any specific land cover type). The normalized distance (z) computes the distance between two random-sampled means, using the mean and standard deviation values. This index is defined as:

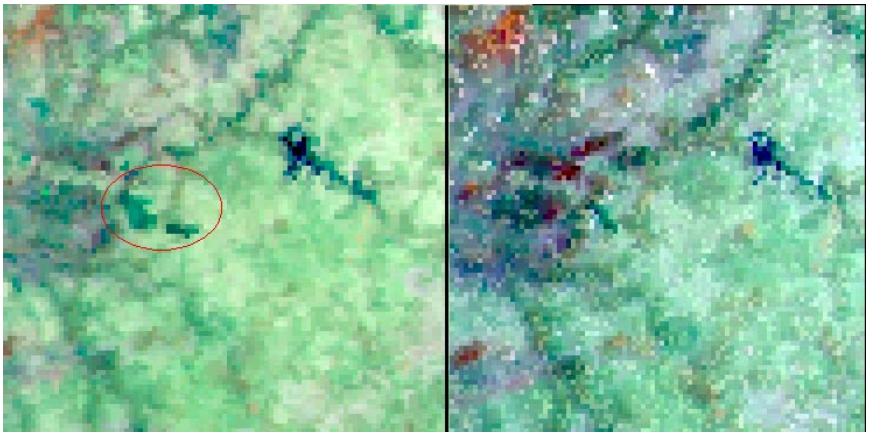

Figure 1: Multitemporal composites: TS-Nadir angle (left); MVC (right)

$$Z_{ab} = (\mu_a - \mu_b) / (\sigma_a - \sigma_b)$$

where μ_a is the mean value for the burned class and μ_b the mean of any other land cover class, and σ_a and σ_b their standard deviations, respectively. This index has been used by several authors to test the discrimination ability of several indices in burned land mapping (Martín and Chuvieco, 2001; Pereira, 1999).

Finally, the transformed divergence was computed to select the spectral band with the highest discrimination power of separating category pairs (i.e. burned areas and any other land cover). This index has been extensively used in classification of remote sensing images (Mather, 1998; Thomas et al., 1987).

3.3 *Temporal analysis*

To analyse the burned land discrimination power of both MODIS and AVHRR data, temporal and spatial analysis were performed. The first one aimed to describe the temporal behaviour of fire-affected areas, with respect to other land covers. The purpose would be to explore which bands or band combinations better separates the temporal change introduced by the fire with respect to other sources of change (harvest, vegetation seasonal trends, etc.). The Corine-Land Cover map of the whole Spain was used to define representative sites of each major land cover. A set of 3x3 pixel windows centred around those sites was used to extract values of each band for the whole study series of images (from May to October, 2001). The burned land site was chosen from a large fire affecting the province of Huesca (Center-North of Spain) in the first week of August. Graphs and statistical indices were derived to identify the most sensitive band for discriminating the temporal change introduced by fire from other seasonal changes affecting other land covers.

4 RESULTS

4.1 *Visual discrimination of burned areas*

Figure 2 shows an example of the incidence of MODIS improved spatial resolution to discriminate burned areas with respect to AVHRR data. The sub-images are centered upon the fire of “Mallos

de Riglos", an important cultural and ecological area in Huesca province that suffers a large forest fire in the first days of August, 2001 that affected 3278 has.

The effect of the spatial resolution is evident in the better characterization of the fire perimeter in the MODIS image, which clearly portrays the differences between the affected area and the surrounding forested lands. The AVHRR composite image makes it possible to discriminate the burned area as well, but with less clarity than with MODIS data. The perimeter is much coarser, and the distinction in areas of less dense forest cover much weaker.

Regarding color quality, the color composite is fairly similar, although the AVHRR image is much more limited to generate visual discrimination scenarios, since it does not have bands in the blue and long short wave infrared (SWIR) wavelengths, which have been demonstrated more sensitive for visual identification of burned areas (Koutsias et al., 2000). Saving this limitation, the color composites of figure 2 include bands in the SWIR (assigned to the red gun), near infrared (green gun) and visible (blue gun) spectral regions. Spectral contrast between burned areas and surrounding covers is clearly more sharp in MODIS than AVHRR composites.

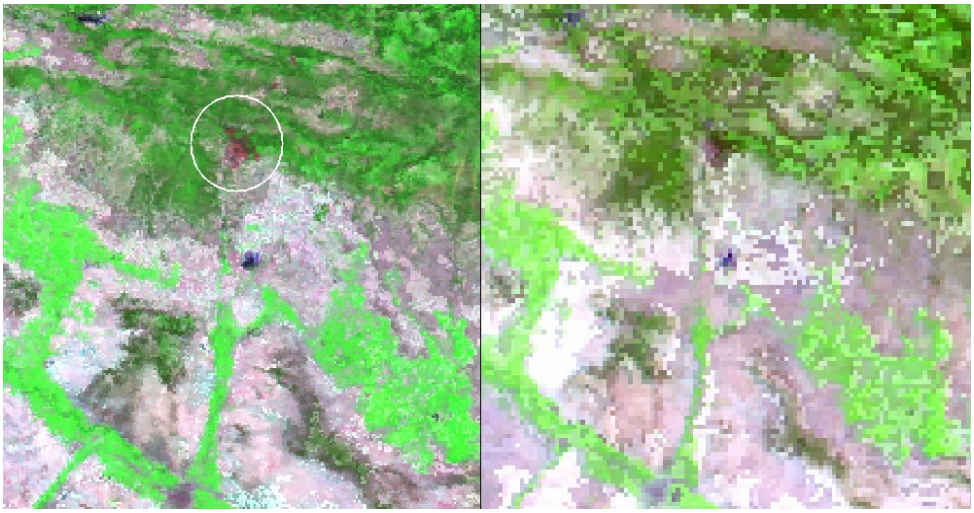

Figure 2: From left to right, MODIS (7/2/1) and AVHRR (3/2/1) color composites of a large forest fire (circled in white) affecting the Pre-Pyrenees mountains of Spain in the first week of August, 2001. The city of Zaragoza is shown at the bottom part of the images, as well as the central section of the Ebro Valley.

4.2 *Spatial discrimination*

Table 2 includes the average z distances between burned land and other land covers. In both MODIS and AVHRR images, the near infrared band (B2) offers the highest average distances, which implies that this spectral band is very sensitive to discriminate burned areas from other land covers, specially from vigorous vegetation (irrigated crops, fruit trees and broad leaf trees mainly). MODIS shows a better sensitivity than AVHRR, with higher distances in B2 and most other channels. It should be remembered than channels 4 and 5 of AVHRR are thermal channels and do not correspond to the spectral wavelengths covered by the MODIS channels processed here.

Table 3 offers a contrasted view, showing the most discriminant channels based on the average transformed divergence. The best and the two best channels have been selected in both MODIS and AVHRR images. This index selects again near infrared (B2) of MODIS as the most single discriminant channel for most combinations of burned area and other land covers, although other bands are recommended to separate burned areas from broad leaf, fruit trees and bare rock. In the case of AVHRR, thermal channels are selected instead of the near infrared band in six out of thir-

teen combinations, while the SWIR band (B3) is selected other three times. For single channels, divergence values are higher for MODIS than for AVHRR images, with the exception of urban, rainfed crops and olive trees.

Table 2: Average Z distances between burned areas and other 13 land covers

	B1	B2	B3	B4	B5	B6	B7
MODIS	2.18	4.16	1.71	2.03	3.05	1.61	1.38
AVHRR	1.71	2.47	1.33	1.40	1.64		

Table 3: Average Transformed Divergence values between burned area and other 13 land covers in MODIS and AVHRR images. The best and the second best discriminant bands are included as well as the divergence value

	MODIS					AVHRR				
Land cover	Diverg	BB[1]	Diverg	BB[1]		Diverg	BB[1]	Diverg	BB[1]	
rainfed	93.16	2	172.35	4	7	147.03	3	141.57	3	5
irrigated	203.21	2	637.28	6	7	129.24	3	204.85	3	5
vineyards	118.17	2	139.44	5	7	114.20	5	174.98	3	5
fruit trees	525.41	5	664.17	6	7	304.70	5	359.28	4	5
olive trees	150.39	2	164.92	2	7	234.13	2	135.84	2	3
broad leaf	162.35	5	602.94	6	7	64.46	5	115.30	2	5
conifer	27.68	2	113.18	1	7	52.49	4	132.87	2	4
grasslands	73.23	2	137.39	1	3	50.53	3	64.94	3	4
shrubland	71.00	2	153.80	5	7	6.56	2	17.80	3	5
bare rock	52.97	3	142.13	4	6	67.09	4	162.36	3	5
sparse-veg	26.14	4	155.86	1	7	10.38	1	34.27	1	3
water	203.41	7	349.37	6	7	0.00	None	0.00	None	
urban	26.37	1	86.61	1	6	430.41	5	873.27	4	5

(1) BB=Best discriminant band

When two bands are considered for divergence measures, the selection of the most discriminant bands shows notably differences from the previous situation. In this case, the divergence takes into account the information provided by the second band not considered in the first one, and therefore in some cases the best single discriminant band is not selected. As far as MODIS images concern, B7, located in the far SWIR, participates in most two-band combinations (ten out of thirteen combinations), which informs about the importance of the SWIR in the discrimination of burned areas, as it was also reported in Koutsias et al. (2000) and Pereira (1999). The second most significant band varies depending on the land covers considered, although a visible band (1, red, or 4, green) is the most frequent option. Indices designed to emphasize the burned signal should, therefore, take into account the SWIR and visible channels.

Regarding AVHRR images, the inclusion of thermal channels notably modifies those conclusions, since the thermal bands are in all cases (with the exception of water and sparse vegetation) selected for the two-band discriminant space. The importance of the thermal channel for burned land mapping has not been frequently emphasized, because this signal is strongly dependent on the time length between image acquisition of fire extinction. In this case, the images were acquired a few days after fire, and therefore the thermal effect of fire is clearly present. On the other hand, the interest of the SWIR channel is also evident in AVHRR images, stressing the importance of this spectral region for burned land mapping.

4.3 *Multitemporal trends*

Discrimination of burned areas may be undertaken with a single post-fire image (or composite), or with time series analysis of images acquired before and after the fire (Pereira et al., 1999). In this second case, the burned areas are identified by analyzing the changes induced by the fire in the spectral reflectance (or temperature), with respect to other changes due to seasonal vegetation trends or man-made alterations (deforestation, harvesting…). The burned areas will be identify when their temporal changes are unique from other time modifications.

To analyze the effect of those changes on MODIS images, figures 3 and 4 include temporal trends of major land covers with respect to burned areas in MODIS data. To simplify the analysis, only the most discriminant bands (B2 and B7) have been selected. B2 shows a clear decrement of reflectance as a result of the fire (first week of August), while other land covers maintain their values without sensible losses thorough the summer (shrubs, coniferous, broadleaf), or show a clear decrement at the beginning of summer (grassland, rainfed crops). Only irrigated crops offers a clear increment of reflectance from Spring to Summer, which agrees with the expected tendencies.

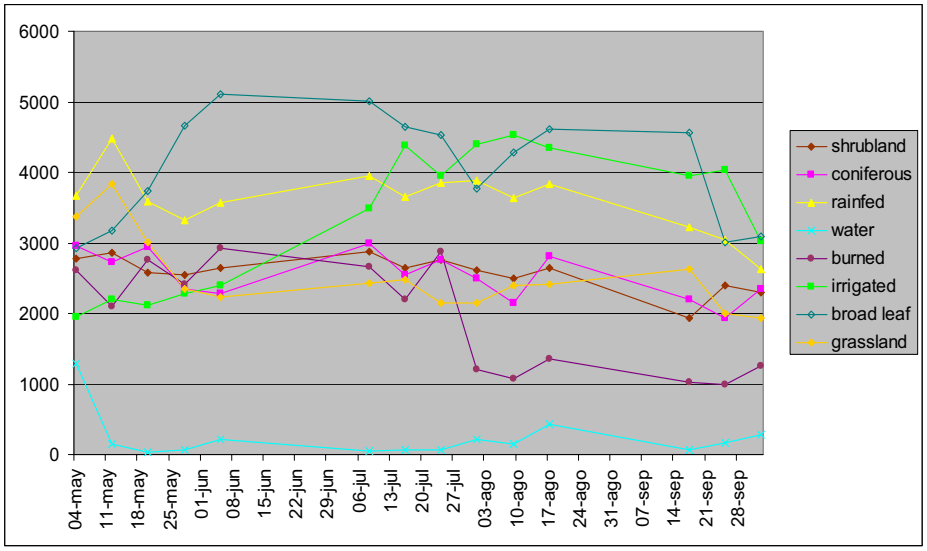

Figure 3: Seasonal evolution of a burned area and other land covers (May – October, 2002) in band 2 (NIR) of MODIS. The vertical scale includes reflectances x 10000.

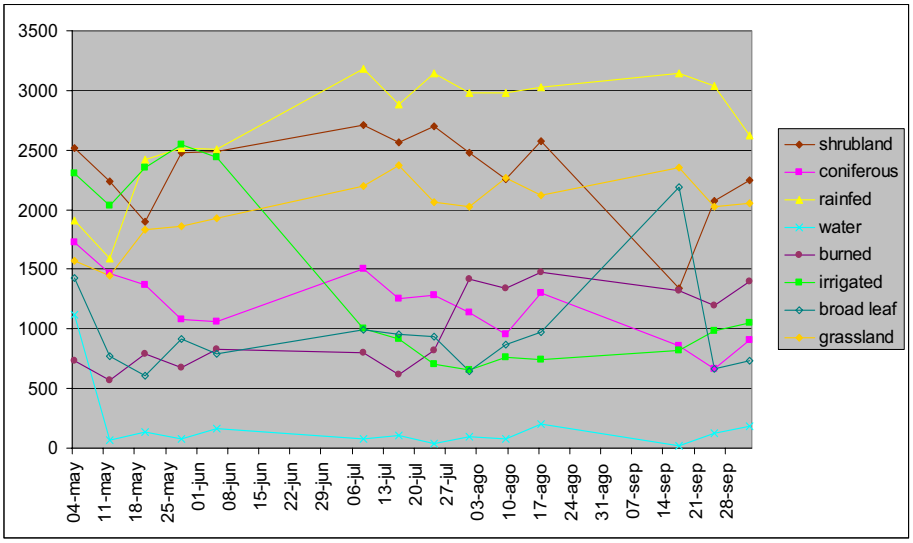

Figure 4: Seasonal evolution of a burned area and other land covers (May – October, 2002) in band 7 (SWIR) of MODIS. The vertical scale includes reflectances x 10000.

With respect to B7, the tendencies are complementary, since burned areas increase their reflectance as a result of fire, while other covers show an stationary trend (coniferous, water, grassland, rainfed), or a clear decrease (shrub, irrigated crops).

5 CONCLUSIONS

Spatial and temporal analysis trends of MODIS and AVHRR data show a clear discrimination power of both sensors to differentiate burned areas, specially when using SWIR and thermal data (when fires are recent) or SWIR and NIR bands.

MODIS data were found more appropriate for burned land mapping, caused by both spatial and spectral resolution.

This analysis should be the basis to define indices specifically adapted to burned land discrimination. They should be based on the most sensitive bands and explore both the spectral and temporal changes introduced by the fire.

ACKNOWLEDGMENTS

The authors greatly acknowledge the support of the SPREAD PROJECT (Contract EVG1-2001-00043). Thanks also to NASA for providing the MODIS images through the EOS Data Gateway Service.

REFERENCES

Bruzzone, L. and Fernández-Prieto, D. (2000), An adaptive parcel-based technique for unsupervised change detection, *International Journal of Remote Sensing*. 21(4): 817-822.

Chuvieco, E. (Ed.) (1999). Remote Sensing of Large Wildfires in the European Mediterranean Basin. Springer-Verlag, Berlin.

Fraser, B.H. and Landry, Z.L. (2000), Spot Vegetation for characterizing boreal forest fires, *International Journal of Remote Sensing*. 21(18): 3525-3532.
Fraser, R.H., Li, Z. and Cihlar, J. (2000), Hotspot and NDVI differencing synergy (HANDS): a new technique for burned area mapping over boreal forest, *Remote Sensing and Environment*. 74: 362-376.
Koutsias, N. and Karteris, M. (1998), Logistic regression modelling of multitemporal Thematic Mapper data for burned area mapping, *International Journal of Remote Sensing*. 19: 3499-3514.
Koutsias, N., Karteris, M. and Chuvieco, E. (2000), The use of intensity-hue-saturation transformation of Landsat-5 Thematic Mapper data for burned land mapping, *Photogrammetric Engineering and Remote Sensing*. 66: 829-839.
Landry, R., Ahern, F. and O'Neil, R. (1995), Forest burn visibility on C-HH radar images, *Canadian Journal of Remote Sensing*. 21: 204-206.
López, M.J. and Caselles, V. (1991), Mapping Burns and Natural Reforestation Using Thematic Mapper Data, *Geocarto International*. 1: 31-37.
Martín, M.P. (1998). Cartografía e inventario de incendios forestales en la Península Ibérica a partir de imágenes NOAA-AVHRR. Tesis Doctoral Thesis, Universidad de Alcalá, Alcalá de Henares.
Martín, M.P. and Chuvieco, E. (1998), Cartografía de grandes incendios forestales en la Península Ibérica a partir de imágenes NOAA-AVHRR, *Serie Geográfica*. 7: 109-128.
Martín, M.P. and Chuvieco, E. (2001), Propuesta de un nuevo índice para cartografía de áreas quemadas: aplicación a imágenes NOAA-AVHRR y Landsat-TM, *Revista de Teledetección*. 16: 57-64.
Mather, P.M. (1998). *Computer Processing of Remotely Sensed Images*, John Wiley & Sons, Chichester.
Pereira, J.M., Sa, A.C.L., Sousa, A.M.O., Martín, M.P. and Chuvieco, E. (1999), Regional-scale burnt area mapping in Southern Europe using NOAA-AVHRR 1 km data. In: *Remote Sensing of Large Wildfires in the European Mediterranean Basin* (E. Chuvieco, Ed.) Eds.), Springer-Verlag, Berlin, pp. 139-155.
Pereira, J.M.C. (1999), A comparative evaluation of NOAA-AVHRR vegetation indices for burned surface detection and mapping, *IEEE Transactions on Geoscience and Remote Sensing*. 37: 217-226.
Thomas, I.L., Ching, N.P., Benning, V.M. and D'Aguanno, J.A. (1987), A review of multi-channel indices of class separability, *International Journal of Remote Sensing*. 8: 331-350.
Trigg, S. and Flasse, S. (2001), An evaluation of different bi-spectral spaces for discriminating burned shrub-savannah, *International Journal of Remote Sensing*. 22(13): 2641–2647.